Academic Journal of International University of Erbil

Journal Homepage: https://ojs.cihanrtv.com/index.php/public

PRINT-ISSN: 2519-6928

Online-ISSN: 3080-7174

Oak Trees Deterioration in Kurdistan Forests: Assessing Climate Change Effects with Fungal Infestation Using Multi-Analytical Methods

Khalat Fadhil Mohammed[1]*, Kamal Kolo[1,2]

[1]Petroleum Geoscience Department, Faculty of Science, Soran, Kurdistan Region, IRAQ

[2]Scientific Research Center (SRC), Soran University, Soran, Kurdistan Region, IRAQ

DOI: https://doi.org/10.63841/iue31642

Received 12 Jul 2025; Accepted 10 Aug 2025; Available online 19 Jan 2026

ABSTRACT:

The observed rapid pace of climate change in Iraq, as well as worldwide, coupled with anthropogenic interventions such as agricultural and urban expansion, is threatening the integrity and sustainability of natural forests. In the Kurdistan Region of Iraq, oak forests constituting nearly 90% of the region's forest cover are exhibiting alarming signs of decline, particularly in the Barzan area, where heartwood decay and hollowing of trunks have become prevalent across young and old trees. This study provides the first detailed multiparametric investigation into oak tree decline in Barzan forests, integrating field observations, SEM-EDX, XRD, and FTIR spectroscopy. FTIR-based indices revealed significant degradation of cellulose and hemicellulose, with lignin-to-cellulose ratios exceeding 1.0 in decayed samples. SEM-EDX analysis confirmed extensive fungal hyphal colonization and localized calcium oxalate biomineralization within heartwood tissues. XRD results showed a progressive decline in cellulose crystallinity index (from 51% in healthy to 35% in severely decayed wood). Tree ring width chronology (1928–2023) showed a declining growth trend, strongly correlating with rising temperatures and declining precipitation in the region. These findings suggest climate-driven fungal decay as the primary mechanism of oak forest deterioration in Kurdistan.

Keywords: Fungal infestation, heartwood decay, oak decline, climate change, Barzan, Kurdistan.

1 INTRODUCTION

Forests are considered one of the most vital ecosystems on Earth, playing a major role in regulating the carbon budget, biodiversity preservation, and providing essential services for both natural systems and human societies. Forests support a wide array of ecological, economic, social, and aesthetic functions, including carbon sequestration, soil protection, hydrologic cycle regulation, and the supply of food, medicine, and timber and covering about 30% of the land area globally [1]. However, the combined impacts of naturally occurring climate change and anthropogenic activities have placed immense pressure on forest health, with significant consequences for ecosystem integrity and function.

1.1 THE GLOBAL CONTEXT OF FOREST DEGRADATION

Historically Oak declines were observed in the 1700s in Germany, the first recorded decline episode in the United Kingdom dates back to the 1920s, a second episode was reported in 1989–1994, and a third from 1997 with no reported end date [2]. The marked increase in atmospheric carbon dioxide levels since 1850 [3] primarily due to anthropogenic activities such as fossil fuel-based industry, deforestation, and land-use-land cover change. This rise in carbon dioxide (CO_2) has intensified climate feedbacks and exacerbated forest stress worldwide. Anthropogenic activities and the increase in population numbers have led to a rise in greenhouse gases (GHG) including CO_2 level, surpassing historical records. Trees and vegetation play a crucial role in storing and sequestering carbon, ensuring that the global concentration rise remains limited to below 2 ppm annually by 2050 [4]. The Climate change is expected to have profound direct and

 *Corresponding author: khalat.mohammed@soran.edu.iq

indirect effects on forest ecosystems. Forest ecosystems are being altered at increasingly rapid rates because of climate and anthropogenic drivers of change [5]. Natural disturbances such as fires, insect outbreaks, and windstorms play crucial roles in forest dynamics [6], but their frequency and severity are being amplified by changing climate conditions.

1.2 FORESTS IN IRAQ AND THE KURDISTAN REGION

In Iraq, natural oak forests, mainly *Quercus spp*., are largely confined to the Zagros and Taurus mountainous areas of the east-northeast and north-northwest of the Kurdistan Region [7]. They comprise approximately 90% of the total forest cover, with the remainder consisting of plantations, pine forests, riverine forests, and mixed stands with species such as *Pistacia khinjuk* and *Crataegus azarolus* [7]. These forests are critical for regional climate resilience, carbon storage, and biodiversity conservation. The health of these forests is increasingly threatened by a convergence of biotic and abiotic factors, including climate change, deforestation, land-use change, and the legacy of conflict and war-related activities during the 1970s-1990s. These factors have disrupted the dynamic equilibrium between the accumulation and decomposition of woody biomass in natural ecosystems [8, 9]. This balance is typically maintained through the activity of diverse microbial communities, with fungi playing a particularly prominent role as decomposers in wood decay and nutrient cycling[9].

1.3 OAK DECLINE: A MULTI-FACETED PROBLEM

Tree diseases and decline are often the result of complex interactions between multiple biotic and abiotic factors, including warm temperatures, drought, pest insects, and pathogens [10, 11]. The incidence and severity of decline events are influenced by the intensity, duration, and frequency of stress events, as well as the ability of opportunistic pathogenic organisms to exploit weakened trees [12]. Oaks (*Quercus spp*.), as primary species in many ecosystems [13], are particularly susceptible to decline, with heartwood decay by fungi representing a major threat to their structural integrity and ecological function.

The process of heartwood decay in oaks is primarily mediated by wood-decay fungi, especially *basidiomycetes*, which colonize the heartwood through wounds, broken branches, or exposed tissues [14]. These fungi use some special enzymes to degrade lignin, cellulose, and other wood components, leading to the development of heart rot and the formation of trunk cavities [15]. While such decay processes are natural components of forest dynamics, their prevalence and severity have increased in recent years, raising concerns about the long-term viability of oak-dominated ecosystems. The resulting heart rot compromises the mechanical stability of trees and creates habitats for a variety of organisms, contributing to nutrient cycling and forest dynamics [16]. The decay is often facilitated by environmental stressors that weaken tree defenses, such as drought, frost, or defoliation by insects [17].

The synergistic interaction between fungi and other biotic agents, such as insects e.g., ambrosia beetles [18] can further exacerbate decay and accelerate tree decomposition, which can also change the structure of plant communities and control the number of hosts [19]. The diversity of fungal communities involved in oak heartwood decay is greater than that previously recognized, with molecular studies revealing a complex assemblage of pathogenic and saprophytic species [20].

1.4 SOIL MINERALOGY AND FOREST HEALTH

Soil mineralogy plays a critical role in forest health, influencing nutrient availability, water retention, and the susceptibility of trees to stress and disease. In the Barzan area, soils exhibit considerable mineralogical diversity, with variations in clay content, carbonate accumulation, and the presence of minerals such as dolomite, lizardite, palygorskite, and sepiolite. These differences reflect the complex geological and geomorphological history of the region and may modulate the response of oak forests to climate change and pathogen pressure.

1.5 DATA GAPS AND STUDY RATIONALE

Despite the ecological and economic importance of oak forests in the Kurdistan Region, there is a paucity of field-based, laboratory-supported research on the causes and mechanisms of oak decline in the region. Existing studies have largely focused on aspects such as the nutritional [21] and mineralogical properties of oak soils [22], the structural diversity of oak stands [23], and the carbon sequestration potential of *Quercus Aegilops* [24]. Recent work has identified the presence of pathogenic fungi such as *Biscogniauxia mediterranea* in *Quercus infectoria* [25], but comprehensive investigations into the interplay between climate change, fungal infestation, and forest health remain limited.

This study aims to address this gap by providing a multiparametric assessment of fungal decay in oak tree heartwood from the Barzan forests, integrating geochemical, spectroscopic, and microscopy techniques. The findings are intended to provide a foundation for future monitoring, research, and management initiatives aimed at safeguarding the region's valuable oak ecosystems.

2 STUDY AREA

2.1 GEOGRAPHICAL AND GEOLOGICAL SETTING

The study was conducted in the Mirgasor district, Barzan area, located 130 km north of Erbil city in the Kurdistan Region of Iraq. Mirgasor includes five sub-districts – Sherwan Mazen, Barzan, Perrin, Mazne and Gorato – as well as 252 villages. Barzan, part of Mirgasor district is near the Iraqi, Iranian and Turkish border junctions. The survey sites were located at the following coordinates: 36.85444° N, 44.08500° E; 36.81761° N, 44.06225° E; 36.80875° N, 44.04485° E; 36.83807° N, 44.11570° E; and 36.82472° N, 44.22117° E in Barzan area (Figur 1).

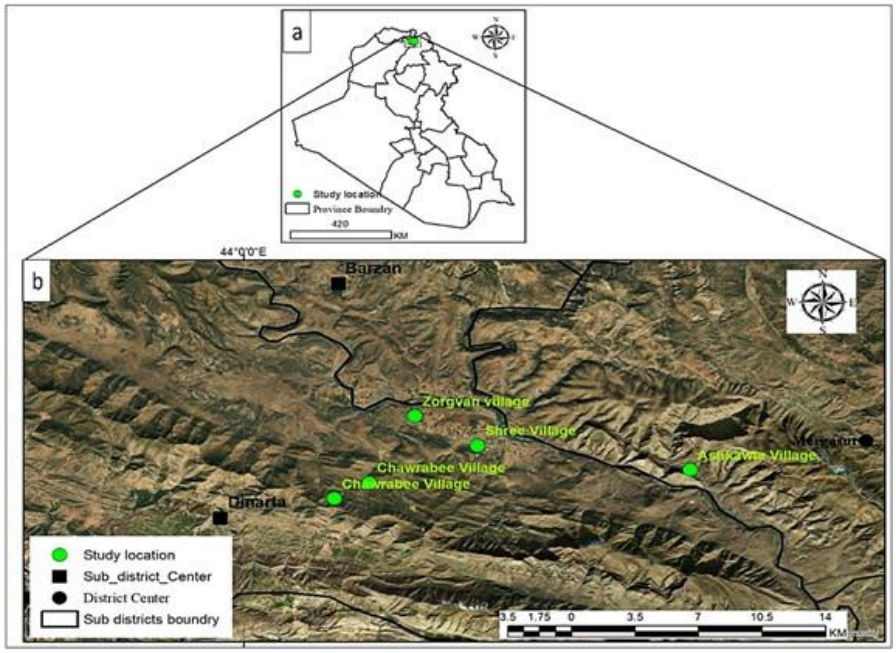

FIGURE 1. (a) general map of Iraq, (b) topographic image of Barzan area with green points, location of study areas.

The region is characterized by rugged terrain, with elevations ranging from 800 to over 2,200 meters above sea level. The climate is continental, with cold winters, early snowfalls, and annual precipitation exceeding 1,000 mm [26]. The geology is dominated by Upper Cretaceous carbonate formations, including the Bekhme, Aqra, Qamchuqa, and Sarmord Formations (Figur. 2), which form the major mountain chains and are separated by synclinal troughs.

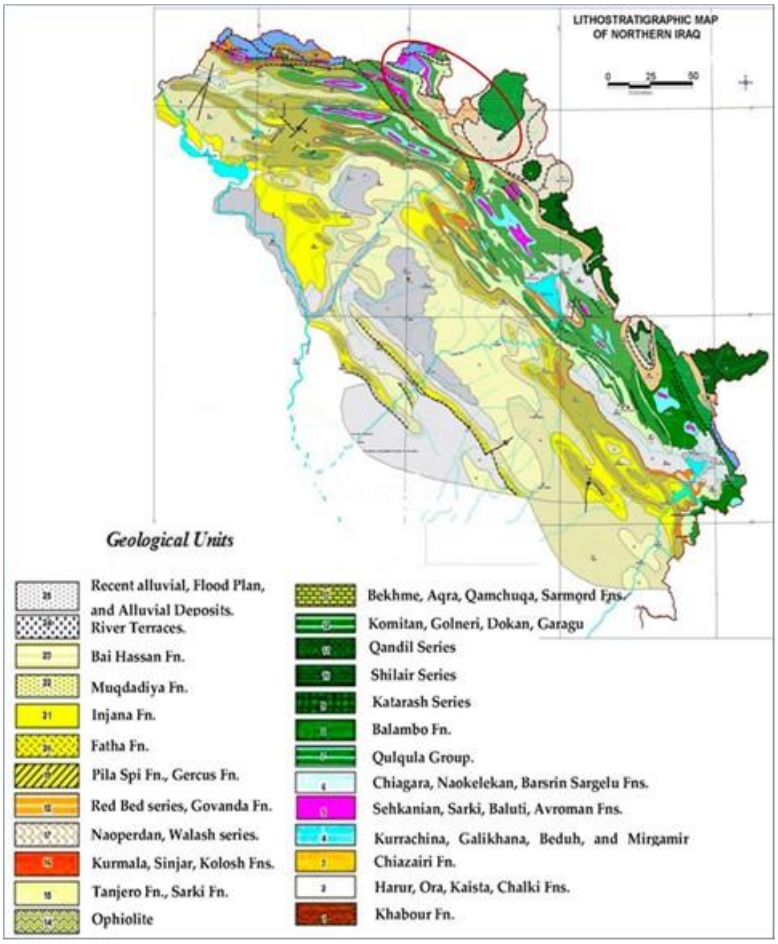

FIGURE 2. Geological map showing the lithological units of the study area (After Stevanovic and Marcovich [27]).

Soils in the area have variable compositions, besides clays [26], they display local variations of dolomitic and serpentine-derived soils, particularly in villages such as Chawrabee, Shree, and Zoragvan. The mineralogical composition of these soils reflects both local bedrock and the transport of ultramafic material from upstream regions, contributing to the heterogeneity of the forest environment.

2.2 FOREST COMPOSITION AND OAK SPECIES

Kurdistan forests are primarily composed of broad-leaved species, mostly oak (Quercus) making up about 90 %, and coniferous forests pine (*Pinus spp.*). Oak trees form the main species of the mountain forests including *Quercus aegilops* (balut) with *Q. infectoria*, and *Q. libani* (dindar) [28]. In the Barzan region, the forest composition includes tree species such as *Quercus aegilops, Q. infectoria* (Fig. 3), and *Pistacia eurycarpa* along with a variety of shrubs and herbaceous plants. Oak trees in the region thrive at elevations between 800 and 1,500 meters, occupying mountain slopes and woodlands across Kurdistan, Syria, Iran, and Turkey, Jordan, Lebanon, southeastern Europe (notably Greece), Palestine, and Cyprus [29]. *Quercus Aegilops* is a deciduous tree that reaches up to 20 meters in height, with lanceolate to ovate leaves and serrated margins [29]. *Q. infectoria* is also deciduous, growing up to 15 meters, with leathery, elliptic-oblong leaves and cylindrical nuts [29]. Both species are adapted to a range of climatic and edaphic conditions but are increasingly threatened by environmental stressors and disease.

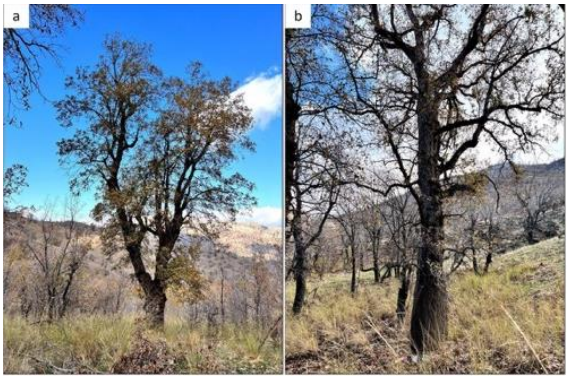

FIGURE 3. Field photos of native oak tree species in Barzan forests (a) *Quercus aegilops* and (b) *Q. infectoria*. Increments borer samples were collected from here and other parts. Photo captured on 28 January 2025, of Increment borer sampling and

3 MATERIAL AND METHODS

3.1 FIELD SAMPLING

Fieldwork was conducted between August 2024 and January 2025 across multiple locations in the Barzan region, including the villages of Zoragvan, Shree, Ashkawta, and Chawrabee. The primary objective was to document patterns of wood decay and collect samples for laboratory analysis. Increment borers were used to extract wood cores from living and fallen trees at a standardized height of 1.3 meters above ground level [30]. Additional samples of bark, leaves, and soil were collected from the vicinity of sampled trees (Fig. 4) (Table 1). Soil samples were obtained from rectangular holes at a depth of 20 cm [31], following the removal of surface soil and debris to minimize contamination. All samples were georeferenced using GPS and labeled for subsequent analysis. In total, multiple wood cores, bark, leaf, and soil samples were collected from each site, with a healthy wood sample and a slab from *Quercus aegilops* included as controls.

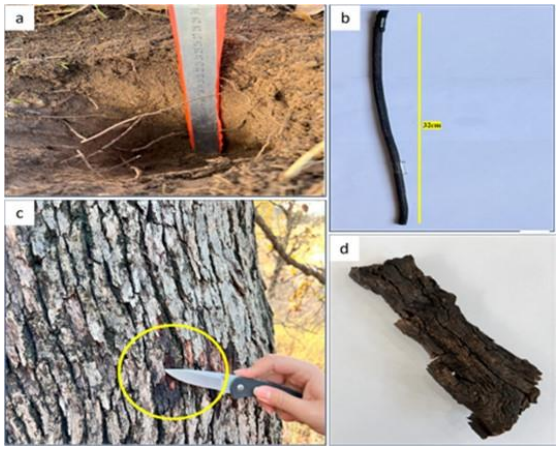

FIGURE 4. Representative sample types collected from oak forests in the Barzan region for multi-analytical investigation of fungal decay and environmental conditions. (a) Soil sampling at 20 cm depth after removal of surface debris. (b) Extracted increment borer core (~32 cm) taken at breast height (1.3 m) from an oak tree to assess internal wood condition. (c) Outer bark of an oak tree, with the sub-bark cambium layer exposed to reveal black fungal infestation indicative of active decay (yellow circle). (d) Severely degraded heartwood fragment detached from the core of a recently felled oak tree, exhibiting advanced fungal colonization and structural breakdown.

Table 1. Sample numbers, types and location.

Sample location	Cores	Decayed wood Samples	Soil	Bark	Leaves	Notes on Cores
Ashkawta Village	1 *(25cm)	1	N/A	N/A	N/A	Incomplete core
Shree Village	2 (50cm) 1 (25cm)	N/A	1	N/A	N/A	All cores incomplete
Zoragvan Village	4 (50cm)	N/A	1	N/A	1	All cores complete (black coloration, potentially indicative of internal decay or possible fungal infection)
Chawra Bee Village	2 (50cm) 1(25cm)	1	3	2	3	All cores incomplete

* Increment borer length

3.2 SAMPLE PREPARATION

3.2.1 WOOD, CORE AND BARK

- Sample Chips were oven-dried in glass beakers at 45–50°C for 24 hours, ground into powder, and used for:
    a. Running FTIR, XRD, analysis on potential biominerals formed through fungal interaction with wood material.
    b. Running direct FTIR, XRD analysis on dried powdered wood for crystallinity indices and composition.
- Thin sections were prepared directly from sliced wood fragments by microtome, and stained with methylene blue, safranine, xylene for light microscope.
- Mineral Extraction: Biominerals formed through fungal interaction were extracted from wood powder using double-distilled water, centrifugation, and ultrasonic treatment for microscopy.
- Wood slices and core chips were variably used in SEM-EDX imaging and elemental mapping for fungal and biominerals detection.

3.2.2 SOIL

Samples were oven-dried in glass beakers at 50 C° for 24 hours and sieved to obtain fine, debris-free powder for XRD mineralogical and elemental analysis.

3.2.3 OAK TREE SLAB

The surfaces of the sample were sanded to ensure a high visibility of the tree ring boundaries. After surface preparation the annual growth rings and ring width were manullay counted.

3.3 Sample Analysis

The X-ray Diffraction (XRD) was used to identify mineral phases in both wood and soil, as well as to assess the crystallinity of cellulose within wood tissues. Data were acquired using a Philipps PANalytical X'Pert PRO MPD Alpha powder diffractometer and processed using High-Score Plus software. Scanning Electron Microscopy (SEM), performed with an FEI Quanta 450 instrument equipped with a Bruker EDS detector, enabled detailed imaging of the wood and core microstructure, elemental analysis of biominerals, and visualization of fungal colonization. Optical microscopy was applied to thin sections of wood, bark, and leaves to evaluate the extent of fungal invasion, tissue degradation, and mineral precipitation. Additionally, Fourier-Transform Infrared Spectroscopy (FTIR) was utilized to investigate the chemical

composition of wood samples specifically cellulose, lignin, hemicellulose, and fungal biominerals using a Shimadzu IRAffinity-1 spectrometer, with spectral data collected across the 500–4000 cm^{-1} range.

4 RESULTS AND DISCUSSION

4.1 SOIL MINEALOGY

XRD analysis of soil samples from Chawrabee, Shree, and Zoragvan villages revealed distinct mineralogical profiles. Chawrabee soils were dominated by dolomite and quartz (Figure 5), indicative of arid to semi-arid conditions and limited leaching of carbonates. Under humid conditions, soil carbonates are susceptible to leaching [32]. But Inadequate precipitation and higher potential evapotranspiration significantly restrict the dissolving and leaching of carbonates from soil [33], and remain in the soil profile knowing that leaching and accumulation of carbonate is controlled by the quantity and temporal distribution of mean annual precipitation [34]. In contrast, soils from Shree and Zoragvan contained lizardite, palygorskite, sepiolite, and quartz (Figure 6), reflecting the transport and deposition of ultramafic material from upstream regions [35]. The presence of these minerals suggests a history of erosion, weathering, and fluvial transport [35], as well as the potential for paleoclimatic reconstruction based on soil mineralogy.

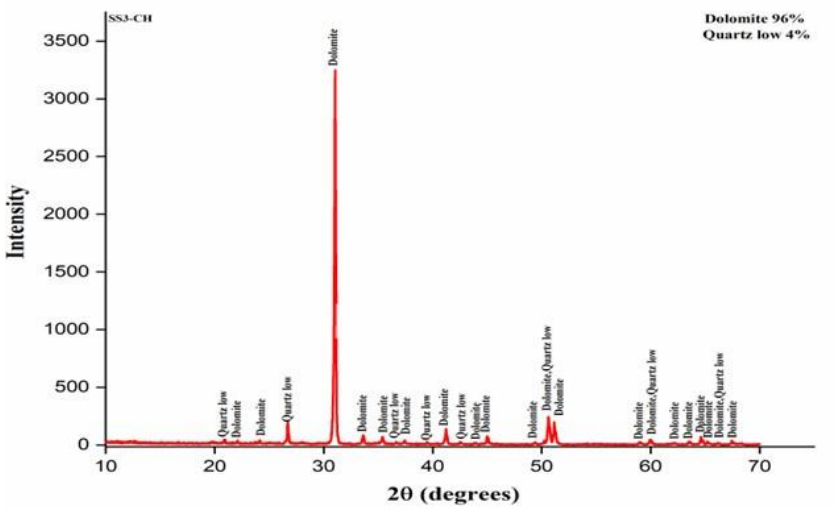

FIGURE 5. X-ray diffractogram of a soil sample from Chawrabee Village, Barzan area. Key diffraction peaks identify dolomite, a sedimentary carbonate mineral, and quartz, commonly derived from the weathering of igneous rocks, hydrothermal activity, or metamorphic processes. The distinct peak positions confirm the dominance of these mineral phases in the local soil profile.

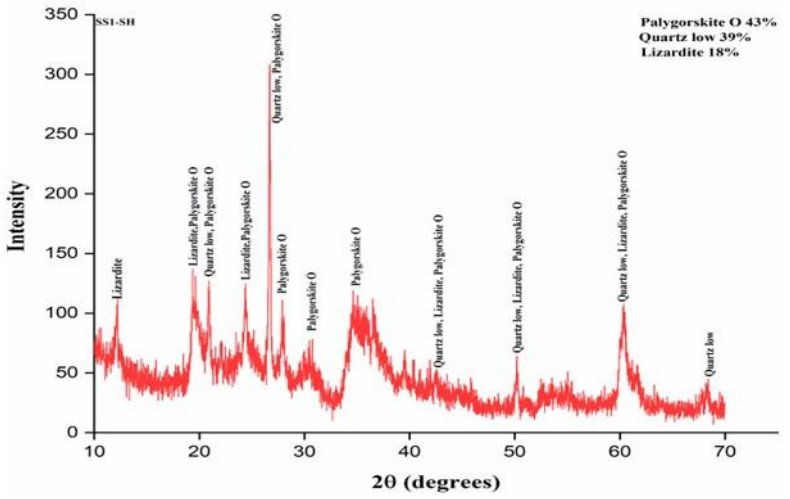

FIGURE 6. X-ray diffractogram of a soil sample from Shree Village, Barzan area. Major mineralogical components identified include palygorskite, a clay mineral typically formed through diagenetic processes in sedimentary environments; quartz, derived from the weathering of igneous rocks, hydrothermal activity, or metamorphism; and lizardite, a serpentine mineral indicative of ultramafic rock alteration under hydrothermal conditions. These minerals reflect the complex geological and depositional history of the region.

4.2 FIELD OBSERVATIONS OF OAK TREE DECAY

All collected oak trees exhibited severe heartwood decay, with increment cores revealing dark, friable, spongy wood and a characteristic odor of rot. Hollow trunks were common, even in trees that appeared externally healthy (Figure 7). In many cases, the increment borer became lodged within the tree, preventing retrieval of a complete core and indicating extensive internal degradation. In cases where the pith was reached, visible symptoms of decay were evident (Figure 8). Root rot and windthrow were observed, with fungal infection evident at the root base of fallen trees (Figure 9). Large trunk cavities, resulting from the degradation of lignin and cellulose by fungal pathogens, were widespread across the study sites (See Figures 10 12, 13, 14).

FIGURE 7. (a) Freshly felled young oak trees showing extensive fungal decay of the heartwood, resulting in complete hollowing of the trunk along a substantial portion of its height. The dark, coal-like heartwood is heavily infested with fungal growth. Photo taken in Ashkawta Village, Barzan area, on 28 October 2024. (b) Core sample extracted from an oak tree with an approximate diameter of 0.8 meters, exhibiting a black-brown discoloration and a strong odor of rot—indicative of advanced fungal degradation. Complete core extraction was unsuccessful due to advanced internal decay; the recovered core segment measured approximately 14 cm in length (red arrow) and showed pronounced fungal infestation. Photo taken in Chawrabee Village, Barzan area, on 28 January 2025.

FIGURE 8. Images of increment borer cores extracted from oak and Fraxinus trees. (a) Healthy Fraxinus (locally known as Bnaw) tree trunk in Kani Shakran, along the Mirgasor road, photographed on 16 August 2024. The core displays intact wood with no visible signs of fungal infection. (b, c) Increment cores extracted from oak trees in Zorgvan Village, Barzan area, on 26 August 2024. Both cores exhibit extensive fungal infection, evident from the blackened heartwood, weakened wood structure, and a pronounced odor of decay. The black discoloration obscures the visibility of tree rings, even after sanding and polishing.

FIGURE 9. (a) Windthrown oak tree uprooted in a cemetery in Zorgvan Village, Barzan area, photographed on 26 August 2024. (b) Core sample from the fallen tree showing pronounced discoloration; the core was entirely encased in black material resulting from advanced fungal colonization. (c) Exposed root system of the same tree, exhibiting severe degradation, blackened decay, and extensive rot.

FIGURE 10. Internal decay of heartwood from freshly felled young oak tree, Chawrabee Village Barzan area (a and b). (c) Fungi is the main agent of the decomposition of lignin and cellulose, producing spongy texture, and resulting in the degradation and eventual loss of heartwood (arrows). Photos captured on 28 November 2024.

4.3 MICROSCOPY AND SEM-EDX ANALYSIS

Microscopic examination of decayed wood revealed extensive structural alteration due to fungal degradation, including collapse and thinning of cell walls, and the presence of dense networks of fungal hyphae. Staining with safranine and methylene blue highlighted areas of residual lignin and cellulose, indicating simultaneous degradation of both components (Figure 11). The observed morphological features were consistent with those characteristics of selective delignification, similar to the findings reported by Srebotnik and Messner [36].

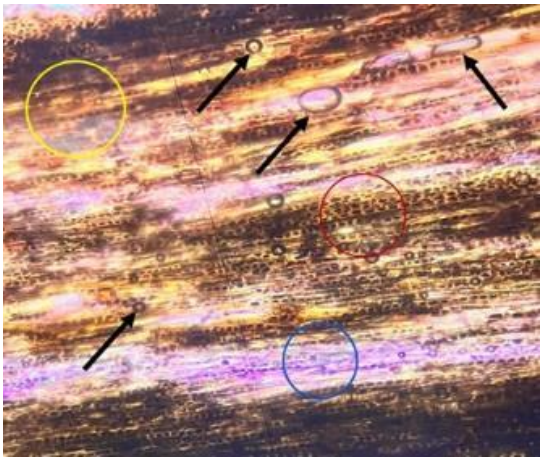

FIGURE 11. Microtome thin section of rotted wood from Ashkawta Village in Barzan area, stained with Safranin and Methylene Blue, shown at 10× magnification. The yellow circle highlights areas of severe anatomical deterioration, characterized by collapsed and distorted cell walls. The blue circle denotes cellulose-rich regions-stained blue following lignin removal by Methylene Blue. Red circle areas represent partial lignification stained by Safranin, indicating intermediate stages of lignin degradation. Areas partially lignified and stained with safranin reveal intermediate lignin breakdown (red circle). These features collectively demonstrate the simultaneous breakdown of both lignin and cellulose. Black arrows point to artifacts, likely air bubbles, introduced during slide preparation.

Wood-decay fungi propagate through wood via microscopic strands known as hyphae, which start off as either fragments of hyphae or germinating spores. These wood-decay fungal strands frequently release oxidizing enzymes that discolor wood and weaken its ability to resist decay [37]. Scanning electron microscopy (SEM) is regarded as a vital method for studying the morphological properties of deteriorated wood at the cell wall level, quantifying damage, and determining the causes of decay patterns [38].

The scanning electron microscopy (SEM) images (Figure 12: A and B) reveal extensive fungal colonization and penetration of the oak heartwood, sometimes in association with insect eggs, suggesting possible insect-fungus interactions. This pattern may resemble ambrosia beetle–fungus interactions, though further confirmation is needed, wherein the fungal growth serves as a nutritional source for the developing larvae [18].

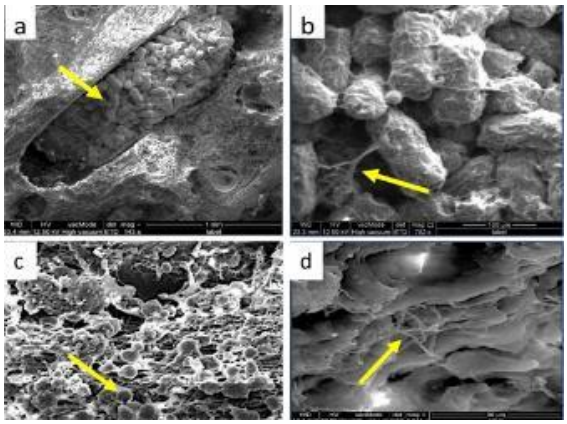

FIGURE 12A. Scanning electron microscopy (SEM) image of decay wood, collected from Ashkawta Village in Barzan area, illustrating a beetle burrow within oak wood. (a) The image shows a cluster of beetle eggs enclosed within a dense mat of fungal hyphae (arrow), likely representing a fungal nest. (b) A magnified view of the burrow highlights the intricate hyphal network—potentially a cultivated fungal matrix—suggestive of a mutualistic relationship between ambrosia beetles and symbiotic fungi such as *Raffaelea*, *Fusarium*, or *Ambrosiella*. These beetles are known to actively inoculate wood with fungal spores during gallery excavation, facilitating the establishment of a fungal "farm" that serves as a nutritional source for their developing larvae. Concurrently, the fungal colonization promotes enzymatic degradation of wood tissues, enhancing the decay process. (c) A separate instance of fungal colonization within oak heartwood from the same locality reveals extensive hyphal proliferation and spore dissemination deep within the wood, indicating an advanced stage of fungal invasion and internal degradation. (d) a detail of wood interlayer invasion and colonization of fungi into the wood micron-sized layers of wood structure.

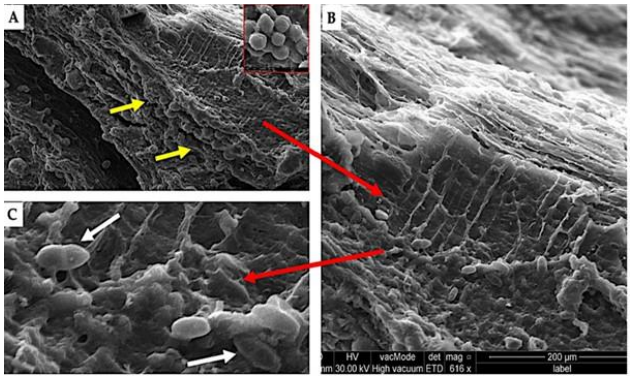

FIGURE 12B. SEM micrographs from the same samples material as above depicting: A) a 3D section of the same sample as above showing the depth of fungal invasion into the decayed wood with hyphae and spores: spherical ~ 25-30um (yellow arrows and figure inset), and uniseptate oval-elliptical forms ~ 30-40 um. The spherical spores are arranged in clusters (inset), single or pairs, showing no ornamentation but rather smooth surfaces covered by visible biofilm material of putative EPS-like matrix observed (extracellular polymeric substance). B and C enlarged view of A showing morphological resemblance to Valsaria rudis noting that further taxonomic work is needed. The uniseptate spores of Valsaris rudis (Dothideomycetes) fungi are known to invade and colonize oak trees (Quercus sp) heartwood [39].

Analysis of increment cores extracted from oak trees (refer to Figure 7b and 8) revealed significant degradation of heartwood in the sampled living tree specimens. In the rare cases where cores covered the complete cross-section of the sampled trees, the heartwood segments were notably blackened and emitted a characteristic odor of decay (Figure 9b). This internal decay can result in the heartwood being entirely or partially absent in extracted cores, as the trees may become hollow due to extensive decay [15]. The results, below display the internal tissue of the heartwood both vertical and horizontal to the core long axis (Figure 13 and Figure 14).

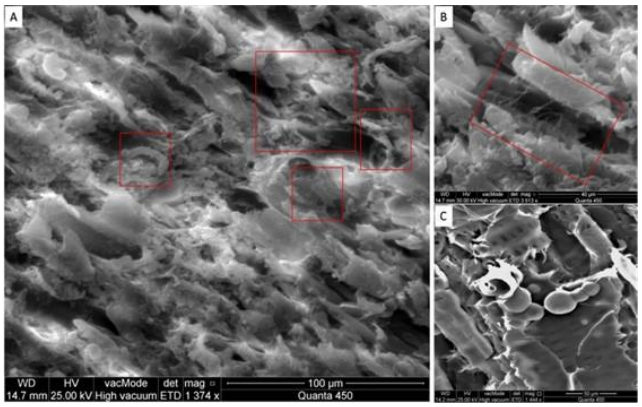

FIGURE 13. Scanning electron microscopy (SEM) images of core sample from oak tree, in Shree Village, Barzan area. Showing longitudinal (A, B) and transverse (C) sections of oak heartwood relative to the core axis. (A) Extensive decay of the heartwood is evident, along with the presence of fungal hyphae and micron-scale geometrically shaped biominerals (highlighted by red rectangles). The left rectangle clearly reveals a fungal hypha fully encrusted with mineral crystals. (B) Enlarged view of the boxed area in panel A, illustrating a network of fungal hyphae spanning a tissue gap. (C) Numerous smooth-surfaced fungal spores resting on the wood matrix. The varying sizes of spherical forms, although not conclusively identified, may represent biseptate spores based on their morphology.

4.4 BIOMINERALIZATION IN DECAYED WOOD

Biomineralization involves the formation of a mineral through the influence of biological processes [40]. From naturally occurring mineral and rock substrates, fungi are known to mobilize or immobilize elements such as Ca, Mn, P, Fe, Mg, S, Al, C, Cd, and Cu [41, 42]. Conversely, the interaction between fungi and wood components primarily cellulose and lignin, and potentially also natural wood resins, appears to facilitate mineral formation. This process is likely driven by biochemical reactions involving fungal organic acids exudates such as oxalic and citric acids (Table 2) [41, 43], leading to the in-situ precipitation of mineral crystals within the tree tissues via fungal organic acid exudates (Figure. 14).

Table 2. Common fungal organic acids exudates and their role [41]

Organic Acid	Function	Common Fungal Genera	Notes
Oxalic acid	Chelation of Ca^{2+}, Fe^{3+}; lignin degradation; crystal formation	Ganoderma, Aspergillus, Armillaria	Dominant acid in white-rot fungi and wood decay
Citric acid	Metal chelation; P solubilization; substrate acidification	Aspergillus, Penicillium	Commercially produced by fungi; aids mineral weathering
Gluconic acid	Lowers pH; solubilizes P and trace metals	Penicillium, Aspergillus	Product of glucose oxidation
Malic acid	Mild chelation; affects pH	Aspergillus, Penicillium	TCA cycle intermediate
Succinic acid	Carbon metabolism; slight acidification	Various filamentous fungi	Less common; contributes to environmental acidification
Fumaric/Itaconic acids	Antimicrobial action; metal complexation	Aspergillus, Ustilago, Rhizopus	Itaconic acid has antimicrobial and industrial uses
Tartaric acid	Minor chelator	Penicillium spp.	Often detected in trace amounts
Lactic acid	Substrate acidification in yeast-like fungi	Zygomycetes, some yeasts	Rare in filamentous fungi

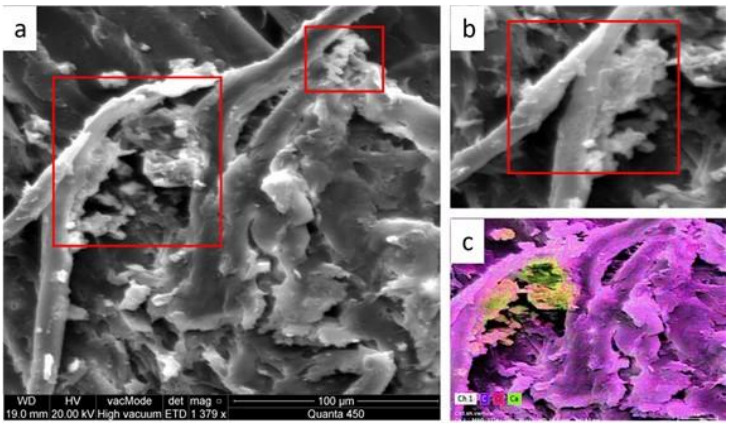

FIGURE 14. SEM-EDX mapping reveals fungal colonization within decayed wood tissues from uncomplete core sample of oak tree in Shree Village, Barzan area (latitudinal-section). Red rectangles in panels (a) and (b) delineate regions of mineral accumulation closely associated with fungal hyphae. Distinct geometric morphologies of micron-scale mineral forms are visible within these zones. (c) The elemental EDX analysis highlights localized calcium-rich mineralization, indicative of oxalate biomineral formation mediated by fungal activity within the colonized wood substrate [43-45].

Fungal exudation of organic acids, particularly oxalic acid, promoted the dissolution and reprecipitation of minerals such as calcium and magnesium oxalates (whewellite, weddellite, glushinskite), as well as carbonates (calcite, dolomite) and struvite, although a broader spectrum of newly formed minerals has been observed to precipitate in accordance with a substrate's specific mineralogy [41, 46]. Experiments involving fungi as plant infections have demonstrated that fungi identify stomatal openings by thigmotropic mechanisms commonly referred to as "contact sensing." [47]. This suggests that mineral formation may proceed independently of direct fungal localization in some cases (Figure 15).

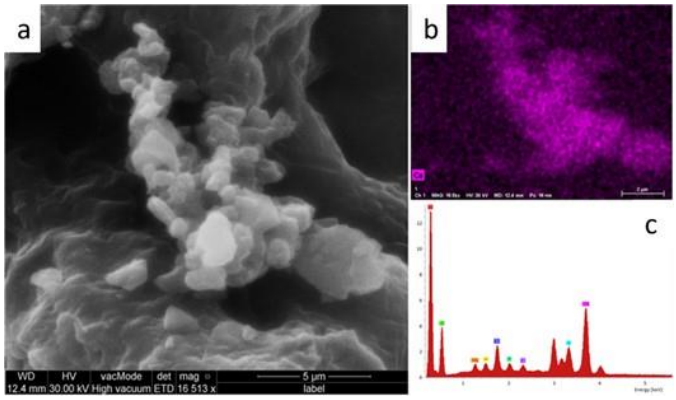

FIGURE 15. SEM-EDX mapping illustrating mineralization within decayed wood tissues from felled oak trees, Ashkawta Village in Barzan area. (a) Clusters of micron-sized minerals with distinct geometric morphologies are observed embedded within the wood matrix, with no apparent spatial association to fungal hyphae. (b) EDX elemental map highlighting calcium (Ca) distribution, where intense bright zones indicate localized Ca enrichment, suggestive of calcium oxalate mineralization. (c) EDX spectrum displaying the elemental composition of the mapped region. Among the analyzed elements, only Ca exhibits pronounced zonation in the total elemental map, while other elements appear uniformly distributed, contributing primarily to background signal.

Inside the bark sample under a light microscope—following the removal of several thin surface layers using a surgical scalpel-revealed filamentous structures that were mineralized (Figures 16 a and b, arrows). Additionally, a substantial amount of minerals was observed, likely formed through fungal interaction with the organic material inside the bark (highlighted by yellow rectangles). The likelihood of external contamination in the bark samples is considered minimal. Mineral crystals were consistently observed along the hyphal structures.

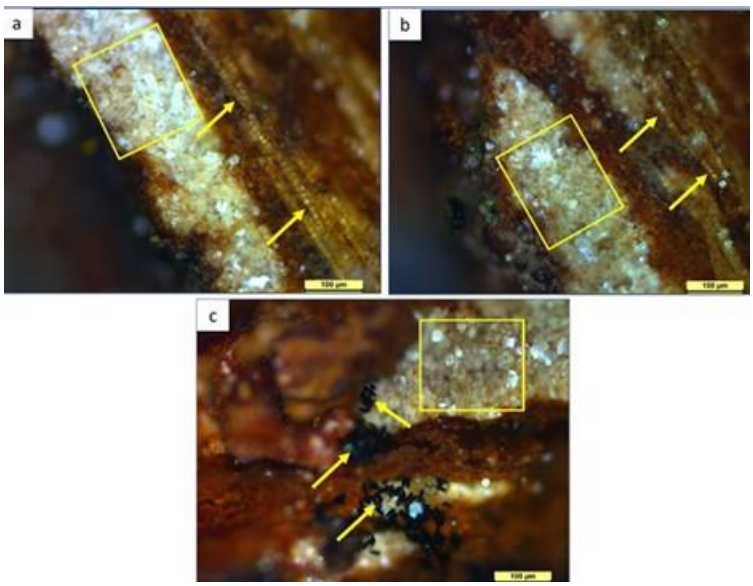

FIGURE 16. Light microscope images reveal localized mineral precipitates inside bark tissue, Chawrabee Village, Barzan area (panels a and b). Yellow rectangles define areas showing dense mineral deposition closely related to filamentous structures suggesting fungal hyphae. Pointing to linear structures that seem to be partially or totally mineralized, arrows indicate hyphal morphology. These findings fit mechanisms of fungal-mediated biomineralization in which fungal colonization encourages the nucleation and expansion of mineral phases inside organic substrates. The spatial relationship between mineralized areas and hyphal structures supports a biogenic origin of the precipitates, perhaps caused by metabolic wastes like oxalate ions, which help to generate calcium-rich mineral phases inside the wood matrix [43]. Panel c (yellow rectangles) also, define areas showing dense mineral deposition. Clusters of black oval structures resembling insect eggs are also visible (yellow arrows). (See Fig. 15.A).

The presence of mineral crystals within the examined decayed wood was further verified by extraction and concentration from crushed decayed wood fragments, sonification in test tubes followed by centrifugation and filtration. Although not all of extracted mineral crystals show typical crystal habits relevant to fungally produced biominerals such as mineral

oxalates, still some forms do (Figure 17A (b-yellow rectangle)). The formation of mineral oxalate crystals, including monohydrate (whewellite) and dihydrate (weddellite) variants, is possible within decayed wood tissues [48, 49] (Figure 17 B). Fungal colonization on the leaf surface is also visible under the microscope (Figure 18).

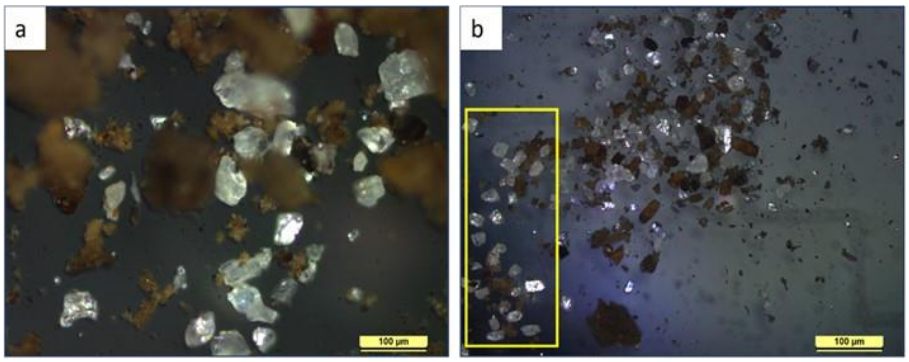

FIGURE 17A. Light microscopy images of mineral crystals extracted from decayed oak wood sample, collected in Ashkawta Village, Barzan area. (a) Displays crystals lacking the well-defined habits typically associated with biominerals. (b) Highlights much better well-formed crystals (yellow rectangle).

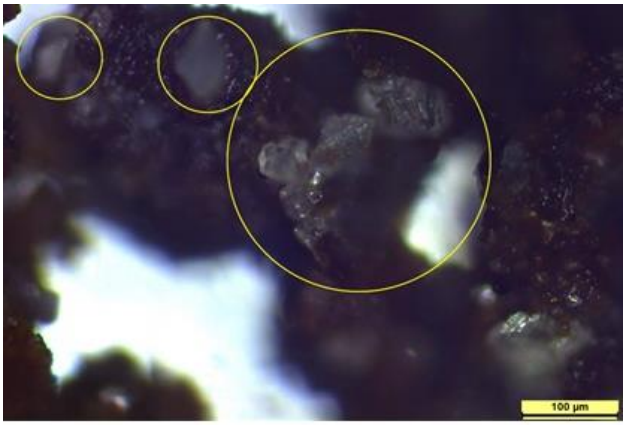

FIGURE 17B. Light microscopy images of mineral crystals extracted from decayed oak wood sample, collected in Ashkawta Village, Barzan area. Prove well-formed shape mineral oxalate crystals (yellow circle). Known to develop as metabolic by-products of fungal activity in lignocellulosic substrates, these crystalline structures fit calcium oxalate monohydrate (whewellite) and dihydrate (weddellite) morphologies [48].

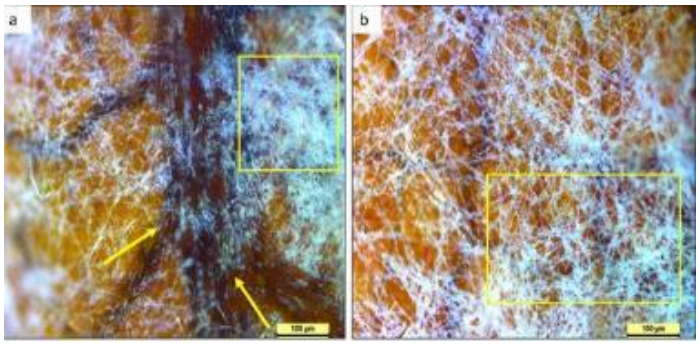

FIGURE 18. Light microscopy images of leaves obtained from Chawrabee Village, 28 November, Barzan region, revealing filamentous fungal hyphae colonizing the leaf surface. Panels (a) and (b) show dense networks of hyphal structures (yellow rectangles) infiltrating and degrading host tissues. Panel (a) shows hyphae distinctly infiltrating the vessels tissues—likely xylem and/or phloem—resulting in structural degradation and tissue discoloration (yellow arrows). Crystalline deposits are observed across the afflicted regions, signifying secondary metabolic or pathogenic processes associated with fungal activity. Scale bars indicate 100 micro-meters.

4.5 FTIR SPECTROSCOPY OF WOOD DECAY

Several characteristic decay parameters were calculated from spectral data spanning 400-4000 cm^{-1}. The results are consistent with fungal rot decay mechanisms, though with several atypical spectral features suggesting complex degradation patterns Table 3. shows the standard FTIR derived indices which are used in assessment of decay levels of tree wood.

Table 3. FTIR absorbance-based wood decay indices and their indicative value ranges for healthy versus fungally degraded wood. The listed absorbance ratios reflect chemical changes associated with the degradation of lignin, cellulose, and hemicellulose. Value ranges are adapted from Pandey & Pitman [50] and Popescu et al [51] and based on FTIR analyses comparing undegraded and fungally degraded wood.

FTIR Index	Formula	Healthy Wood Range	Fungal-Decayed Wood Range	Indication
Lignin-to-Cellulose Ratio	1510 cm^{-1}/898 cm^{-1}	0.30 - 0.65	0.70 - 2.50	Higher values indicate preferential degradation of cellulose by fungi
Carbohydrate Index	1370 cm^{-1}/1510 cm^{-1}	1.40 - 2.20	0.60 - 1.30	Lower values indicate carbohydrate depletion during fungal decay
Carbonyl Index	1730 cm^{-1}/1510 cm^{-1}	0.50 - 0.90	1.00 - 2.50	Higher values indicate oxidation processes during fungal decay
Crystallinity Index	1375 cm^{-1}/2900 cm^{-1}	0.80 - 1.10	0.40 - 0.75	Lower values indicate degradation of crystalline cellulose regions
Hydroxyl/Aromatic Ratio	3400 cm^{-1}/1510 cm^{-1}	0.8-1.2	1.5– 2.5	Lower values indicate loss of hydroxyl groups associated with cellulose and hemicellulose during fungal decay (fungal type plays active role)
Hemicellulose Degradation Index	1730 cm^{-1}/1370 cm^{-1}	0.30 - 0.50	0.80 - 1.60	Higher values indicate preferential hemicellulose degradation
Syringyl/Guaiacyl Ratio	1325 cm^{-1}/1268 cm^{-1}	Species-dependent	Typically decreases in white rot	Changes indicate lignin unit modifications
Cellulose Integrity Index	1160 cm^{-1}/898 cm^{-1}	4.50 - 7.00	2.00 - 4.00	Lower values indicate cellulose chain scission

On the other hand, (Table 4), summarizes the primary functional groups and vibrations identified from the FTIR spectrum. The characteristic peaks correspond well to the major constituents of wood: cellulose, hemicellulose, lignin, and possible extractives.

It is worth noting that the following wavenumbers are used interchangeably during assessment of wood integrity and decay as they are attributed to similar functional groups within wood composition:

- *3400 cm^{-1}: Broad O–H stretch, similar to 3330 cm^{-1}, often used interchangeably.*
- *1375 cm^{-1}: C–H deformation, overlaps with 1370 cm^{-1}, typical for cellulose and hemicellulose.*
- *1325 cm^{-1}: Syringyl ring breathing and C–O stretch, associated with lignin (especially hardwoods) and cellulose.*
- *1268 cm^{-1}: Guaiacyl ring breathing and C–O stretch, characteristic of lignin (especially softwoods).*
- *1505 cm^{-1}: Aromatic C=C stretch, closely related to 1510 cm^{-1}, both are lignin markers.*
- *1160 cm^{-1}: C–O–C asymmetric stretch, already present in (Table 4).*

In order to assess the level of wood integrity samples HW1, WS1, WS2 collected from oak trees in Barzan Area, several standard FTIR-based spectroscopic indices (Table 3) were calculated from the absorbance spectrum [50, 52-55].

FTIR analysis of healthy and decayed wood samples identified characteristic changes in chemical composition associated with fungal degradation. Healthy wood exhibited strong carbohydrate and cellulose peaks (Table 5) (Figure 19), while

decayed samples showed reduced carbohydrate indices, increased lignin-to-cellulose ratios, and diminished hemicellulose signals (Table 6) (Figure 19). The disappearance of the 898 cm^{-1} cellulose band and elevated crystallinity indices in decayed wood indicated selective degradation of amorphous cellulose and hemicellulose, with crystalline cellulose and lignin relatively preserved (Table 7) (Figure 19). below gives direct evidence to the changes in peaks intensity as degradation progresses along the three samples (Figure 24). These patterns are consistent with advanced fungal decay mechanisms and provide molecular evidence of wood decomposition. These observations are in good conformity with XRD diffractograms of the same three samples, marking these two methodologies as quite reliable tools to assess and measure wood quality.

Table 4. Wavenumbers/functional groups assignment for FTIR wood analysis

Wavenumber (cm^{-1})	Assignment	Component
3400	O–H Stretch	(Cellulose, Hemicellulose)
3330	O–H Stretch	(Cellulose, Hemicellulose)
2900	C–H Stretch	(Cellulose, Lignin)
1730	C=O Stretch	(Hemicellulose, Extractives)
1600	Aromatic C=C	(Lignin)
1510	Aromatic C=C	(Lignin)
1505	Aromatic C=C	(Lignin)
1425	CH_2 Scissoring	(Cellulose)
1375	C–H Deformation	(Cellulose, Hemicellulose)
1370	C–H Deformation	(Cellulose, Hemicellulose)
1325	Syringyl Ring Breathing/C–O Stretch	(Lignin, Cellulose)
1268	Guaiacyl Ring Breathing/C–O Stretch	(Lignin)
1160	C–O–C Asym. Stretch	(Cellulose, Hemicellulose)
1050	C–O Stretch	(Cellulose, Hemicellulose)
895	β-Glycosidic Linkages	(Cellulose)

Table 5. Calculated indices of wood sample HW a healthy wood from the native FTIR absorbance spectrum.

Index	Value	Interpretation
Lignin-to-Cellulose Ratio (1505/898)	0.4476	Falls well within the healthy wood range (0.30–0.65). Indicates normal cellulose content and no preferential lignin enrichment, which is a key sign that fungal degradation has not occurred.
Carbohydrate Index (1370/1505)	1.7555	This is within the healthy range (1.40–2.20), reflecting abundant carbohydrate content (cellulose and hemicellulose) relative to lignin. Supports the conclusion of well-preserved polysaccharides.
Carbonyl Index (1730/1505)	0.732	This value falls within the healthy range (0.50–0.90), suggesting minimal oxidative degradation of lignin and hemicellulose. No major carbonyl accumulation due to fungal decay is present.
Crystallinity Index (1375/2900)	1.755	A value significantly above the typical healthy threshold (>1.1) indicates high cellulose crystallinity. This is consistent with intact cellulose microstructure, showing no sign of structural disruption from decay.
Hydroxyl/Aromatic Ratio (3400/1505)	1.942	Above the range for healthy wood. In health wood, this may reflect normal hydration state during sample preparation rather than decay.

Table 6. Calculated indices of wood sample WS1-Ash a degraded wood from the native FTIR absorbance spectrum.

Index Name	Formula	Value	Healthy Range	Decayed Range	Interpretation
Lignin-to-Cellulose Ratio	1505/893	0.984	0.30–0.65	0.70–2.50	High: Suggests cellulose loss and lignin enrichment, a signature of fungal decay.
Carbohydrate Index	1370/1510	1.148	1.40–2.20	0.60–1.30	Low: Indicates depletion of carbohydrate content (cellulose + hemicellulose), typical of advanced fungal decay.
Carbonyl Index:	1730/1505	0.233	0.50–0.90	1.00–2.50	Low: Reflects oxidation of hemicellulose, ester, and carbonyl accumulation—sign of active biodegradation.
Crystallinity Index	1375/2921	2.545	0.80–1.10	0.40–0.75	Very high: Suggests the loss of hemicellulose and amorphous cellulose, consistent with fungal attack. leaving behind a more crystalline cellulose framework
Hydroxyl/Aromatic Ratio	3400/1510	0.820	0.8-1.2	1.5– 2.5	Close to lower bound, indicating no significant loss of hydroxyl groups yet or reduced carbohydrate content.
Hemicellulose Degradation Index	1730 / 1370	0.188	0.3–0.50	0.8-1.6	Very low: Clear sign of preferential hemicellulose degradation, typical of fungal decay.
Total Crystallinity Index (TCI)	1372/670	0.471	0.80–1.10	0.40–0.75	Low → indicates cellulose degradation. The ratio reflects ordered, tightly packed cellulose chains relative to amorphous regions and disordered hydrogen bonding. This value confirms fungal degradation of crystalline cellulose.
Lateral Order Index (LOI)	1430/898	1.083	1.10-1.50	0.90-1.10	Near-normal → some lateral cellulose order retained. The ratio reflects lateral packing of cellulose microfibrils relative to glycosidic bon disruption.

Table 7. Calculated indices of wood sample WS2-Ch a degraded wood from the native FTIR absorbance spectrum.

FTIR Index	Formula	Value	Interpretation
Lignin-to-Cellulose Ratio	1505 / 897	1.10	897 cm^{-1} peak absent or severely diminished – not interpretable, suggests moderate to advanced decay
Carbohydrate Index	1370 / 1505	1.194	Falls within the fungal-decayed wood range (0.60–1.30). This confirms carbohydrate depletion, indicating degradation of cellulose and hemicellulose, which are more susceptible to microbial attack than lignin.
Carbonyl Index	1730 / 1505	0.315	Clearly above the decay threshold (>1.00). High carbonyl absorbance suggests oxidative degradation of lignin and hemicellulose (Faix, 1991). This is typical fungal or oxidative decay.
Crystallinity Index	1375 / 2921	2.535	Very high for a moderate-advanced wood sample
Hydroxyl/Aromatic Ratio	3400 / 1505	1.20	Above the healthy range (0.70-1.00). This ratio suggests increase in hydroxyls from hemicellulose or cellulose breakdown
Hemicellulose Degradation Index	1730 / 1370	0.268	Suggests mild hemicellulose oxidation, less intense decay progression. Also, possibly due to poor peak resolution at 1730cm-1.
Total Crystallinity Index (TCI)	1372/670	0.45	Reflects loss of crystalline cellulose structure. Strongly supports moderate to advanced fungal degradation.
Lateral Order Index (LOI)	1430/898	1.20	Indicates some preservation of lateral cellulose chain order. Suggests the degradation has not yet completely disrupted crystalline alignment.
Cellulose Integrity Index	1160/898	1.081	Extensive cellulose depolymerization: Indicative of moderate to advanced fungal decay

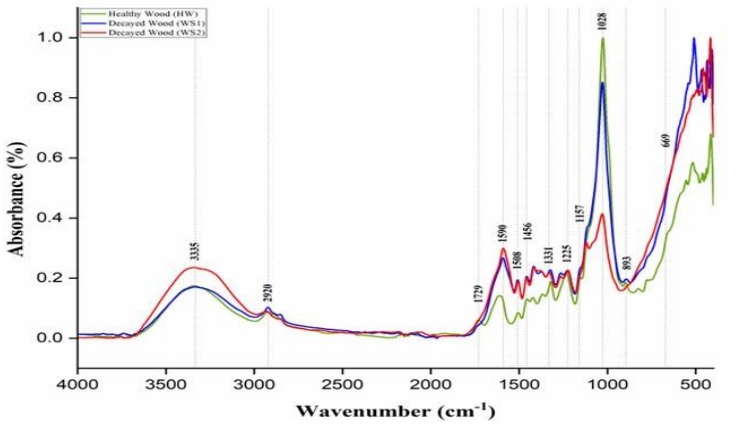

FIGURE 19. FTIR absorbance spectra (4000–450 cm^{-1}) of three wood samples: healthy heartwood (HW), moderately decayed wood (WS1), and severely decayed wood (WS2) from oak trees in the Barzan area. The spectra reveal progressive chemical changes associated with fungal degradation. Important spectral differences include reduced cellulose associated peaks, and elevated carbonyl (1729 cm^{-1}), lignin and (1510 cm^{-1}) aromatic signatures. The broadening and intensity shifting of the hydroxyl peak reflects degradation of hydroxyl-rich components. The significant reduction in the β-glycosidic linkage band (~898 cm^{-1}) in decayed samples highlight advanced cellulose degradation.

4.6 XRD ANALYSIS AND CRYSTALLINITY INDEX

The X-ray diffraction (XRD) data from wood specimens showed the levels of decay through calculation of the crystallinity index (CI). As a natural composite material, wood primarily consists of cellulose, hemicellulose, and lignin. Here, we selected three wood samples collected from oak trees that presented various levels of wood degradation (heartwood showing brown-black discoloration) and one visibly healthy heartwood sample where it shows no degradation, decay or change in color as a control and comparison. The samples are labeled WS1- Ash, WS2-Ch for the degraded wood and HW-1 for the healthy wood.

The superposed XRD diffractograms of the three wood samples show two primary peaks characteristic of cellulose I. The major crystalline peak (200) at 2θ = 22.7° with an intensity of 2042, 1273, 847 counts respectively. A secondary

crystalline peak (101) (or a doublet (101)/(10$\bar{1}$) at 2θ = 14.89° with an intensity of 1,189 counts. The amorphous region at in the region of 18-19 2θ are 1001, 733, 550 counts respectively. These peak positions are consistent with the typical diffraction pattern of cellulose I in wood samples, where the (002) peak is generally observed around 22-23° and the (101) peak around 15-16° 2theta (Fig. 20 and 21).

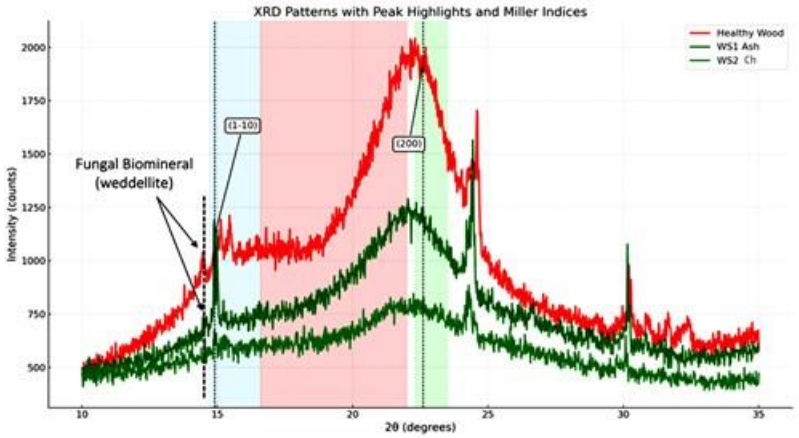

FIGURE 20. XRD diffractograms of decayed heartwood (WS-1, WS-2) and healthy heartwood (HW-1), highlighting reduced intensity in degraded specimens compared to the higher intensity of the undegraded wood. The crystalline cellulose is typically around 15 and 22.6 2θ positions, for 15 2θ which show sharp peak, and is reliable with the literature accounts [56, 57]. Segal et al [58] and French and Santiago Cintrón [59], identified the amorphous region at approximately 18° 2θ. French [60] indicated that the amorphous contribution is typically observed between 17° and 21° 2θ, overlapping with crystalline peaks. This range is especially relevant for samples with lower crystallinity or those affected by decay. The amorphous cellulose region is between 18-22 2θ positions which is acceptable according to literature. Observe the hump region in the healthy wood that gradually decreases in intensity in the decayed wood creating the amorphous cellulose valley.

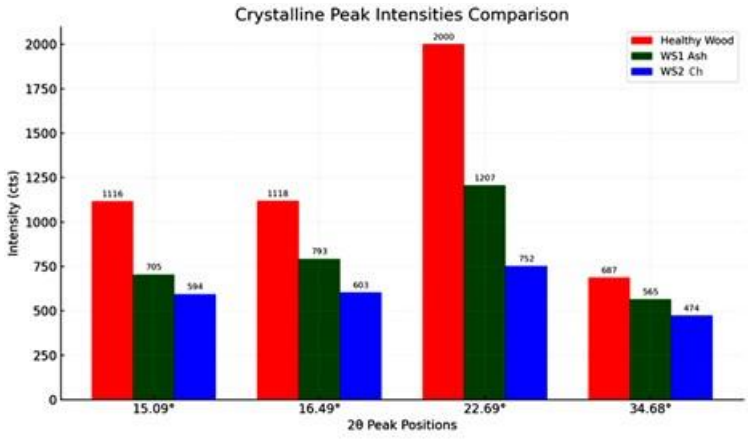

FIGURE 21. Histogram comparing crystalline peak intensities at selected 2θ positions for healthy (HW-1) and decayed (WS-1, WS-2) wood. The healthy specimen exhibits consistently higher peak intensities, reflecting greater crystallinity and structural preservation, while the decayed samples show a marked reduction in intensity across all peaks.

XRD profiles of wood samples showed progressive loss of crystallinity from healthy to decayed wood, quantified by the Crystallinity Index (CI). Healthy wood had a CI of 51%, while decayed samples dropped to 42% and 35%, indicating substantial cellulose degradation (Table 8).

Table 8. Crystallinity index (CI) values for three of the samples that were being analyzed showed a progressive decline, which indicated that the crystalline phases had experienced structural degeneration from the beginning.

Sample	I_{200} (Intensity)	I_{200} (2θ)	I_{am} (Intensity)	I_{am} (2θ)	Crystallinity Index (CI%)
Healthy Wood	2042.0	22.30°	1001.0	18.46°	50.98%
WS1 Ash	1273.0	22.35°	733.0	18.13°	42.42%
WS2 SH	847.0	22.25°	550.0	18.02°	35.06%

Principal Component Analysis (PCA) of XRD data further distinguished decay stages, with PC1 explaining over 95% of variance, reflecting structural deterioration (Fig. 22). These findings corroborate the FTIR results and provide a robust framework for assessing wood quality and decay.

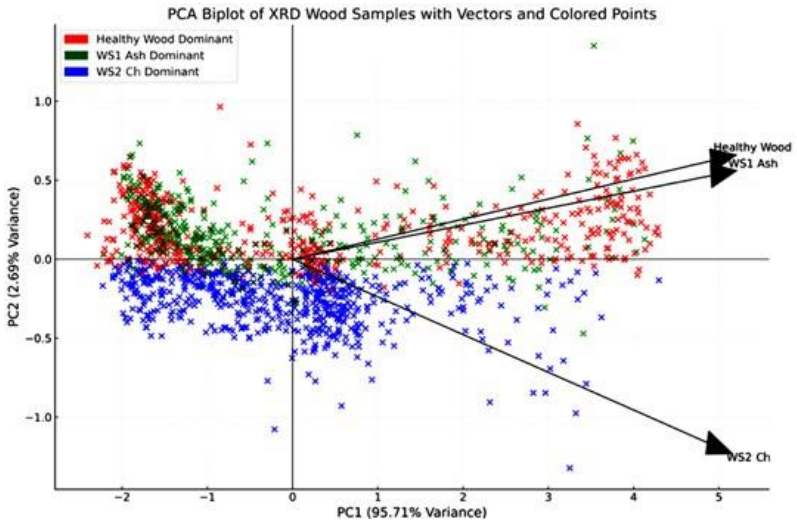

FIGURE 22. Scattered bi-plot of the 2θ positions plotted in Principal Component (PC) space. Their location shows how the XRD pattern intensities at different angles vary relative to each other. Loading vectors showing how strongly each wood sample (Healthy Wood, WS1-Ash, WS2-Ch) influences the distribution of points along the PC axes (PC1 and PC2). The red clusters show domination by health wood pattern; the green and blue clusters are dominated by WS1-ash and WS2-ch samples. The vectors show how strongly is sample WS2-ch deviating from the others. The small angle between Healthy and WS1-ash indicate positive correlation. While the higher angle of WS2-ch vector indicates a negative correlation caused by greater decay.

4.7 MECHANISMS OF OAK DECLINE IN BARZAN FORESTS

Forest decline arises from complex interactions between abiotic stressors such as drought, heat, frost, pollution, and nutrient imbalance and biotic agents, including fungi, insects, and bacteria. These stresses impair photosynthesis, water transport, and carbohydrate storage, weakening trees physiologically [61, 62]. Climate change amplifies these effects by increasing vapor pressure deficit, drought frequency, and pest outbreaks, leading to large-scale forest die-off and reduced ecosystem resilience [63, 64]. Moreover, the risk of disease introduction and spread through international plant trade, combined with the intensifying effects of both current and future climate change, is elevating the incidence and impact of tree diseases particularly those associated with decline syndromes [65]. In the Kurdistan Region elevated temperatures and changing precipitation patterns are expected to foster the growth of fungi and the deterioration of wood. The resulting decay compromises the mechanical integrity of trees, increases their susceptibility to windthrow and mortality, and creates certain habitats for a variety of organisms. Moreover, the precipitation of biominerals within decayed wood and

bark tissues highlights the role of microbial-mineral interactions in forest ecosystems. Fungal exudation of organic acids mobilizes metal ions and promotes the formation of oxalate and carbonate minerals, which may influence nutrient cycling, soil formation, and tree health. The diversity of biominerals observed in this study reflects the complex geochemical environment of the Barzan forests and underscores the need for further research into the ecological significance of these processes. The results of this study provide compelling evidence for a climate-driven, fungal-mediated decline of oak forests in the Barzan area. The widespread occurrence of heartwood decay, hollow trunks, and trunk cavities, even in externally healthy trees, points to a hidden but severe threat to forest health and stability.

4.8 CLIMATE CHANGE SIGNATURE

Climate change is a key driver of oak decline in the Kurdistan Region, as evidenced by rising temperatures, altered precipitation patterns, and increased frequency of drought and extreme events. These conditions favor the proliferation of pathogenic fungi and oomycetes, intensify insect-fungus interactions, and weaken tree defenses against biotic and abiotic stressors. The observed mineralogical diversity of soils in the Barzan area may modulate the response of oak forests to climate change, with implications for tree vulnerability and ecosystem resilience. The temporal changes in recorded temperatures and precipitation in Kurdistan for the period 1901-2024 (Source: World Bank, 2025. See figure 25) align well with general climate change trends observed across the Mediterranean region. Recent climate assessments indicate that the Mediterranean basin is experiencing significant warming trends, with temperatures rising faster than the global average [66, 67]. Climate projections suggest increases in both the frequency and intensity of heatwaves, contributing to heightened ecological and socio-economic vulnerabilities [68]. Concurrently, precipitation patterns have become increasingly variable with an overall declining trend, particularly during summer months, thereby exacerbating drought risks and water scarcity [66, 68]. These shifts toward more extreme and unstable climate conditions are expected to intensify stress on both natural ecosystems and agricultural systems, particularly in semi-arid zones where water availability is already limited [68, 69]. This combination of factors leads to increased vegetation stress in marginal semi-arid environments. While these regional climate trends are well documented, this study utilized long-term temperature and precipitation datasets measured at two locations in the Kurdistan Region—Dohuk and Erbil—in conjunction with tree ring width measurements obtained directly from a well-developed oak tree slab collected from the Barzan area. The analyzed slab exhibits predominantly concentric growth patterns with minimal growth anomalies related to tree positioning (Fig. 23). However, detailed dendrochronological analysis is beyond the scope of this study, which focuses specifically on climate-related aspects of the tree ring data.

FIGURE 23. *Quercus aegilops* tree slab from Alka Village, Barzan area. Felled in 2023.

Figure 24 displays the temporal trend of tree ring width growth as a time series spanning 1928-2023, revealing a general decline in growth rates. Even when accounting for age-related growth factors, the trend demonstrates a consistent decline over time. Temperature plots and trend projections for both the Dohuk and Erbil regions show consistent increases projected into the future, while precipitation trends indicate a negative trajectory (Fig. 25). Fig. 26 represents the decrease in tree growth in warmer and dryer years. Drought or heat is associated with ring width decreasing, indicating climate stress as the main source to growth changes in the oak specimens. This points to trees in semi-arid Mediterranean conditions becoming more and more sensitive indicators of climate change. Although these results are necessarily limited by the single tree sample from the study area, they indicate that a clear climate signature is embedded within the

sampled oak tree growth patterns, suggesting the tree is experiencing climate stress consistent with broader Mediterranean regional trends.

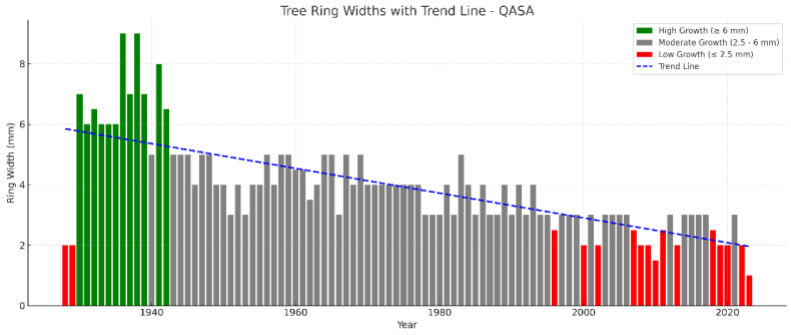

FIGURE 24. Annual tree ring widths (mm) of oak tree from Barzan area for 1928–2023 time series. This pattern illustrates temporal decline in growth interpreted in this work as climate driven decline. It shows periods of above-average growth (green bars), reflecting favorable environmental conditions. Average or stable growth (Gray bars). Reduced growth, typically associated with stress or drought (red bars). The linear trend line shows the overall long-term growth tendency.

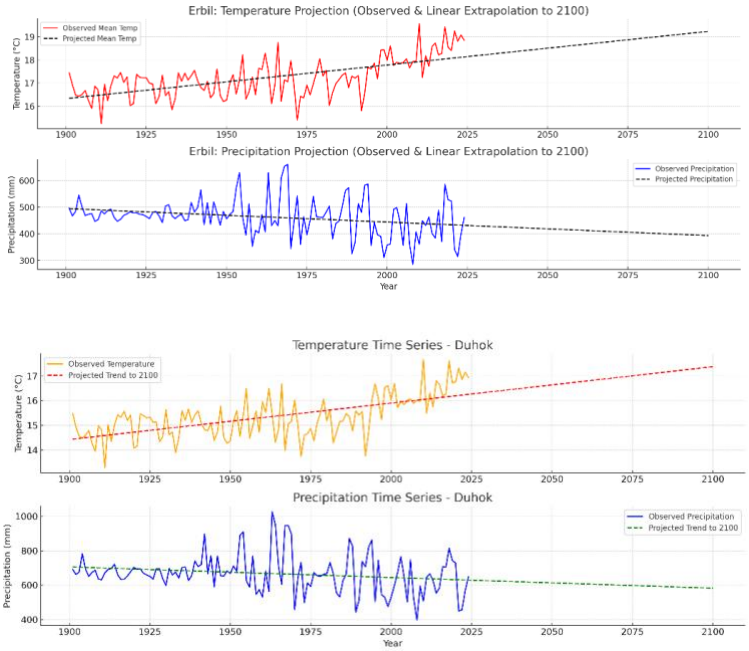

FIGURE 25. Projected temperature and precipitation records on the Dohuk and Erbil regions for period 1901–2024 (Source: The World Bank. Data available at: https://climateknowledgeportal.worldbank.org/country/iraq/climate-data-historical.org). The figure reflects a steady rise in annual average temperatures and a decreasing change in annual precipitation especially during recent decades.

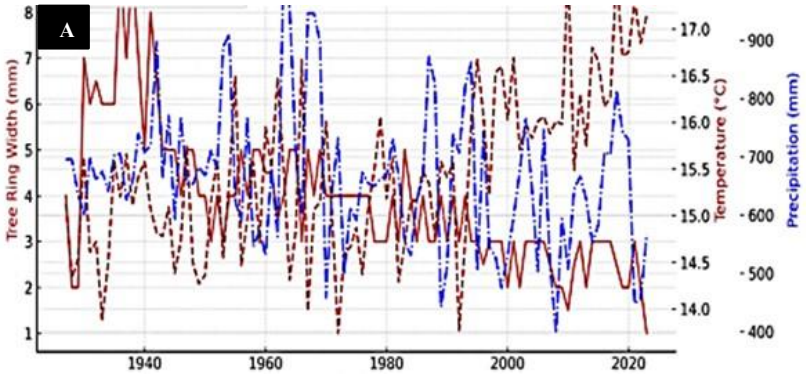

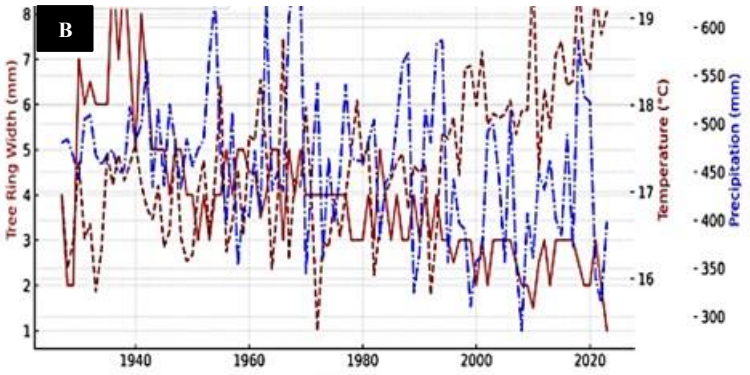

FIGURE 26. A and B. Annual tree-ring width (mm) of oak tree slab (1928–2023) with overlaid temperature (°C) and total annual precipitation (mm) data for Erbil (A) and Duhok (B) (1901–2024). The figure demonstrates a negative relationship between temperature increase and tree growth, while showing a positive relationship between precipitation and ring width.

In the last decades, climate change and its related environmental disturbances have favored the appearance of disease outbreaks caused by plant pathogenic microorganisms [70]. Regional climate data indicate a steady increase in average annual temperature and modifications to rainfall patterns, particularly in the northeast of Iraq [71, 72]. In the entire Mediterranean region, future climate change is likely to intensify drought conditions in this region [73]. The Palmer Drought Severity Index (PDSI) calculated for the period 1950-2012 indicated periods severe drought slightly wet conditions [71]. The Kurdistan region's historical climatic statistics from 1901 to 2021 show an increase in annually mean and minimum temperatures in all regions. There is a relatively small drop in annually mean precipitation across all provinces. Kurdistan, Iraq, has experienced significant climatic change since the 1950s, with prominent trends showing shifts in temperature and rainfall patterns. The average annual temperature has steadily risen over time, at a rate of approximately 0.7°C each century. Additionally, there have been modifications to the annual rainfall, especially in the northeast, where it has increased at a rate of roughly 2.4 mm per month each Century (Source: UNDP: *United Nations Development Programme* report, 2024). These trends are consistent with broader patterns of climate-driven forest decline observed in the Mediterranean Basin, Europe, and Asia. In Mediterranean, several research investigations show that high temperatures and excessive precipitation lead to the spread of pathogens and infection. In particular *for Phytophthora cinnamomi* [74] and *Phytophthora ramorum* [75, 76]. Also, Ambrosia beetles, which are connected to diseases and the degradation of oak trees, are more common in areas with warmer climates[77].

European oak decline is also, influenced by climatic changes, heavy rains, floods, and pests. Phytophthora genus pathogens cause soil saturation, damage roots, and drought. Insect defoliators and mildew infections worsen tree mortality, with secondary insects and root pathogens being the primary causes [78]. In Iran, it is considered that, one of the main reasons for oak decline is drought, which increases fungal aggression and intensifies their destructive effects, leaving oak seedlings more susceptible to abiotic stressors[79, 80]. The interaction between drought, heat stress, and pathogen pressure is particularly pronounced in oak forests, where the loss of structural and functional diversity can have cascading effects on ecosystem services and biodiversity.

4.9 IMPLICATION FOR FOREST MANAGEMENT AND CONSERVATION

The findings of this study have important implications for forest management, conservation, and climate adaptation in the Kurdistan Region and beyond. The hidden nature of heartwood decay and fungal infestation underscores the need for regular monitoring and early detection of decline symptoms, even in trees that appear externally healthy. The integration of advanced analytical techniques, such as SEM-EDX, XRD, and FTIR, provides a powerful toolkit for assessing wood quality, identifying decay mechanisms, and guiding management interventions. Targeted strategies for mitigating oak decline should include the protection of forest soils, the management of wounds and root damage, the control of pest and pathogen outbreaks, and the promotion of tree species and genotypes with enhanced resistance to stress and disease. Restoration efforts should prioritize the conservation of genetic diversity, the maintenance of ecosystem services, and the adaptation of forest management practices to changing climatic conditions.

The results of this study are consistent with previous research on oak decline and fungal decay in other regions, including Europe, the Mediterranean, and Asia. The mechanisms of heartwood decay, the role of fungal enzymes, and the formation of trunk cavities have been well documented in the literature[14, 15, 41, 62, 81]. However, the integration of geochemical, spectroscopic, and microscopy techniques in this study provides a more comprehensive understanding of the processes underlying oak decline in the Barzan forests. The identification of biomineralization processes and the characterization of soil mineralogy represent novel contributions to the field, with potential implications for the study of forest health, nutrient cycling, and biogeochemical interactions. The findings highlight the importance of interdisciplinary approaches in addressing complex ecological problems and underscore the need for continued research and collaboration.

CONCLUSIONS

This study provides the first comprehensive, field- and laboratory-based assessment of widespread, climate-driven fungal decay in oak forests of the Barzan area, Kurdistan Region of Iraq. The decline of oak forests in the Barzan region reflects a multifactorial case driven by the combined effects of climatic stress, fungal pathogenesis, and soil mineralogical influences. The integration of field surveys, dendrochronology, and laboratory analyses including SEM-EDX, FTIR spectroscopy, and XRD the study revealed progressive heartwood decay, extensive fungal colonization, and in situ biomineralization within affected trees. Climate records from the region show a pronounced warming trend since the mid-20th century, accompanied by increased precipitation variability and declining moisture availability in recent decades. Tree ring chronologies demonstrate significant growth suppression beginning around 1980, with a clear correlation between rising temperatures, precipitation deficits, and reduced radial growth. These patterns highlight climate-mediated stress as a primary driver of forest decline. The interaction between temperature and moisture stress appears to compromise tree hydraulic function and defense responses, thereby facilitating fungal invasion and colonization.

Microscopic and chemical analyses confirmed multiple fungal decay mechanisms, including features characteristic of brown rot (preferential cellulose degradation), white rot (simultaneous lignin and cellulose breakdown), and soft rot in moisture-rich tissues. SEM imaging revealed fungal hyphae penetrating wood cell walls and forming boreholes, often associated with calcium oxalate deposits byproducts of fungal metabolism and potential host defensive responses. XRD analysis showed declining cellulose crystallinity in decayed samples, while FTIR spectra indicated elevated lignin-to-cellulose ratios, reflecting selective loss of polysaccharides during decomposition. The strong alignment between FTIR and XRD results demonstrates the effectiveness of combining spectroscopic and structural techniques to quantify wood degradation severity. The association of dendrochronological evidence with regional climate data points to an accelerating decline of oak health in response to ongoing warming. These stress conditions particularly during drought years reduce the tree's capacity to maintain defense systems, while simultaneously enhancing fungal metabolic activity and pathogenicity. This creates a feedback loop in which climate stress weakens host resilience, enabling deeper fungal colonization and accelerating internal wood decay.

The observed mineralogical transformations, especially calcium oxalate precipitation, illustrate a complex biogeochemical interplay between fungal metabolism, host tissue degradation, and environmental conditions. Importantly, many of the infected trees displayed minimal external symptoms, revealing a hidden internal vulnerability that threatens long-term forest stability, ecosystem services, and carbon storage capacity in semi-arid environments. These findings underscore the urgency of implementing forest health monitoring, early fungal detection, and soil quality assessment strategies. Future research should focus on microbial community profiling, insect–fungus interactions, and the ecological consequences of fungal-driven biomineralization. This study provides a preliminary foundational reference for oak forest conservation in the face of climate change and demonstrates the value of multi-analytical approaches in diagnosing and understanding complex forest decline syndromes.

FUNDING

This research received no external funding.

ACKNOWLEDGEMENT

We thank the Scientific Research Center and the Center of Climate Change Studies of Soran University for laboratory and technical support, and the local forestry authorities in Barzan area for their assistance during the fieldwork.

CONFLICTS OF INTEREST

The author declares no conflict of interest.

DATA AVAILABILITY

The data underlying this article will be shared on reasonable request to the corresponding author.

REFERENCES

[1] R. Hassan & R. Scholes, Vol. 1: Current state and trends. Washington, DC [etc.]: Island Press, 2005.

[2] J. Gibbs, Dieback of pedunculate oak (no. 22). 1999.

[3] M. E. Mann, R. S. Bradley, & M. K. Hughes, "Northern hemisphere temperatures during the past millennium: Inferences, uncertainties, and limitations," Geophysical research letters, vol. 26, no. 6, pp. 759-762, 1999.

[4] M. Dangulla, L. Abd Manaf, & M. M. Aliero, "The contribution of small and medium diameter trees in West African Savanna to regional biomass and carbon pools," Academia Environmental Sciences and Sustainability, vol. 2, no. 1, 2025.

[5] G. M. Lovett, M. Weiss, A. M. Liebhold, T. P. Holmes, B. Leung, K. F. Lambert, D. A. Orwig, F. T. Campbell, J. Rosenthal, D. G. McCullough, & R. Wildova, "Nonnative forest insects and pathogens in the United States: Impacts and policy options," Ecological Applications, vol. 26, no. 5, pp. 1437–1455, 2016.

[6] R. Seidl, D. Thom, M. Kautz, D. Martin-Benito, M. Peltoniemi, G. Vacchiano, J. Wild, D. Ascoli, M. Petr, J. Honkaniemi, & M. J. Lexer, "Forest disturbances under climate change," Nature Climate Change, vol. 7, no. 6, pp. 395–402, 2017.

[7] M. Nasser, "Forests and forestry in Iraq: prospects and limitations," The Commonwealth Forestry Review, pp. 299-304, 1984.

[8] J. M. Nash, M. A. Vadeboncoeur, G. G. McGee, C. W. Woodall, & R. D. Yanai, "Biomass accumulation in trees and downed wood in northern hardwood forests: Repeated measures of a successional chronosequence in New Hampshire, USA," Canadian journal of forest research, vol. 54, no. 4, pp. 431-446, 2023.

[9] F. W. Schwarze, "Wood decay under the microscope," Fungal biology reviews, vol. 21, no. 4, pp. 133-170, 2007.

[10] M. E. Harmon, J. F. Franklin, F. J. Swanson, P. Sollins, S. V. Gregory, J. D. Lattin, N. H. Anderson, S. P. Cline, N. G. Aumen, J. R. Sedell, & G. W. Lienkaemper, "Ecology of coarse woody debris in temperate ecosystems," Advances in Ecological Research, vol. 15, pp. 133–302, 1986.

[11] T. Gentilesca, J. J. Camarero, M. Colangelo, F. Ripullone, A. Nole, & A. Nolã, "Drought-induced oak decline in the western Mediterranean region: an overview on current evidences, mechanisms and management options to improve forest resilience," IForest, vol. 10, no. 5, pp. 796-806, 2017.

[12] D. B. Houston, "The shift and share analysis of regional growth: a critique," Southern Economic Journal, pp. 577-581, 1967.

[13] A. O. Conrad, E. V. Crocker, X. Li, W. R. Thomas, T. O. Ochuodho, T. P. Holmes, & C. D. Nelson, "Threats to oaks in the eastern United States: Perceptions and expectations of experts," Journal of Forestry, vol. 118, no. 1, pp. 14–27, 2020.

[14] F. H. Berry & F. F. Lombard, Basidiomycetes Associated with Decay of Living Oak Trees, vol. 413. Broomall, PA: U.S. Department of Agriculture, Forest Service, Northeastern Forest Experiment Station, 1978.

[15] N. J. Brazee & D. C. Burcham, "Internal decay in landscape oaks (Quercus spp.): Incidence, severity, explanatory variables, and estimates of strength loss," Forests, vol. 14, no. 5, p. 978, 2023.

[16] Y. Fukasawa, "Ecological impacts of fungal wood decay types: A review of current knowledge and future research directions," Ecological Research, vol. 36, no. 6, pp. 910-931, 2021.

[17] I. Millers, D. S. Shriner, & D. Rizzo, History of hardwood decline in the eastern United States. US Department of Agriculture, Forest Service, Northeastern Forest Experiment , 1989.

[18] J. Hulcr & R. R. Dunn, "The sudden emergence of pathogenicity in insect–fungus symbioses threatens naive forest ecosystems," Proceedings of the Royal Society B: Biological Sciences, vol. 278, no. 1720, pp. 2866-2873, 2011.

[19] A. P. Møller, "Parasitism and the regulation of host populations," Parasitism and ecosystems, vol. 75, pp. 43-43, 2005.

[20] J. A. Glaeser & K. T. Smith, "Decay fungi of oaks and associated hardwoods for western arborists," Western Arborist. Winter 2010: 32-46., pp. 32-46, 2010.

[21] K. I. Saleem, K. H. Abdullah, K. F. Saadallah, H. I. Abdullah, & R. O. Khalo, "A Nutritional Comparison Study of Three Oaks Species Grown in Gara Mountains," Diyala Agricultural Sciences Journal, vol. 13, no. 2, pp. 63-70, 2021.

[22] A. Abdullah, A. Esmail, & O. Ali, "Mineralogical properties of oak forest soils in Iraqi Kurdistan region," Iraqi Journal of Agricultural Sciences, vol. 50, no. 6, 2019.

[23] M. Haidari, N. Shabanian, R. H. Haidari, & M. Bazyar, "Structural diversity of oak forests in Kurdistan Province (Case study: Oak forest)," IOSR Journal of Pharmacy and Biological Sciences, vol. 4, no. 3, pp. 37-43, 2012.

[24] M. Obeyed, Z. Akrawee, & Y. Mustafa, "Estimating aboveground biomass and carbon sequestration for natural stands of Quercus aegilops in Duhok province, Iraqi," J Agric Sci, vol. 51, no. 10.36103, 2020.

[25] A. Nagham & A. Samir, "First Report of Biscogniauxis mediterranae As Endophytic Fungi Associated with Quercus infectoria from A Mountainous Area In Kurdistan Region, Iraq," Egyptian Academic Journal of Biological Sciences. C, Physiology and Molecular Biology, vol. 16, no. 2, pp. 17-27, 2024.

[26] P. G. Mohammed, A. M. A. Mohammed, & N. M. Abdulrahman, "Impact of Abiotic Factors on growth of Quercus aegilops and Quercus infectoria in Mergasour Natural Forest–Erbil–Iraq," Zanco Journal of Pure and Applied Sciences, vol. 35, no. SpC, 2023.

[27] Z. Stevanovic & M. Markovic, "Hydrogeology of Northern Iraq. Vol. 1. Climate, hydrology, geomorphology & geology. Vol. 2. General hydrogeology and aquifer systems," 2004.

[28] S. E. Shahbaz, S. S. Abdulrahman, & H. A. Abdulrahman, "Use of Leaf Anatomy for Identification of Quercus L. Species Native to Kurdistan-Iraq," Science Journal of University of Zakho, vol. 3, no. 2, pp. 222-232, 2015.

[29] S. A. Ahmad & S. Salih, Qara Dagh mountain plant field guide. American University of Iraq, Sulaimani (AUIS) Press, 2019.

[30] O. D. Diller, "The relation of temperature and precipitation to the growth of beech in northern Indiana," Ecology, vol. 16, no. 1, pp. 72-81, 1935.

[31] D. James & K. Wells, "Soil sample collection and handling: Technique based on source and degree of field variability," Soil testing and plant analysis, vol. 3, pp. 25-44, 1990.

[32] P. W. Birkeland, Soils and geomorphology. 1984.

[33] D. L. Royer, "Depth to pedogenic carbonate horizon as a paleoprecipitation indicator?," Geology, vol. 27, no. 12, pp. 1123-1126, 1999.

[34] M. Egli & P. Fitze, "Quantitative aspects of carbonate leaching of soils with differing ages and climates," Catena, vol. 46, no. 1, pp. 35-62, 2001.

[35] J. Cuadros, J. L. Diaz-Hernandez, A. Sanchez-Navas, A. Garcia-Casco, & J. Yepes, "Chemical and textural controls on the formation of sepiolite, palygorskite and dolomite in volcanic soils," Geoderma, vol. 271, pp. 99-114, 2016.

[36] E. Srebotnik & K. Messner, "A simple method that uses differential staining and light microscopy to assess the selectivity of wood delignification by white rot fungi," Applied and environmental microbiology, vol. 60, no. 4, pp. 1383-1386, 1994.

[37] W. C. Shortle & K. R. Dudzik, "Wood decay in living and dead trees: a pictorial overview," Gen. Tech. Rep. NRS-97. Newtown Square, PA: US Department of Agriculture, Forest Service, Northern Research Station. 26 p., vol. 97, pp. 1-26, 2012.

[38] Y. Bouramdane, M. Haddad, A. Mazar, S. Aît Lyazidi, H. Oudghiri Hassani, & A. Boukir, "Aged Lignocellulose Fibers of Cedar Wood (9th and 12th Century): Structural Investigation Using FTIR-Deconvolution Spectroscopy, X-Ray Diffraction (XRD), Crystallinity Indices, and Morphological SEM Analyses," Polymers, vol. 16, no. 23, p. 3334, 2024.

[39] N. N. Wijayawardene, A. Mešić, A. Pošta, Z. Tkalčec, & M. Thines, "Outline of Fungi and fungus-like taxa–2021," 2022.

[40] S. Weiner & P. M. Dove, "An overview of biomineralization processes and the problem of the vital effect," Reviews in mineralogy and geochemistry, vol. 54, no. 1, pp. 1-29, 2003.

[41] G. M. Gadd, "Fungal production of citric and oxalic acid: importance in metal speciation, physiology and biogeochemical processes," Advances in microbial physiology, vol. 41, pp. 47-92, 1999.

[42] G. M. Gadd, "The geomycology of elemental cycling and transformations in the environment," Microbiology spectrum, vol. 5, no. 1, pp. 10.1128/microbiolspec. funk-0010-2016, 2017.

[43] G. M. Gadd, "Geomycology: biogeochemical transformations of rocks, minerals, metals and radionuclides by fungi, bioweathering and bioremediation," Mycological research, vol. 111, no. 1, pp. 3-49, 2007.

[44] K. Kolo, E. Keppens, A. Préat, & P. Claeys, "Experimental observations on fungal diagenesis of carbonate substrates," Journal of Geophysical Research: Biogeosciences, vol. 112, no. G1, 2007.

[45] K. Kolo & A. Préat, "In Vitro Experimental Observations on Fungal Colonization, Metalophagus Behavior, Tunneling, Bioleaching and Bioweathering of Multiple Mineral Substrates," Minerals, vol. 13, no. 12, p. 1540, 2023.

[46] K. Kolo & P. Claeys, "Rock surface diagenetic biosignatures induced by fungal-carbonate substrate interactions as life indicators," in Finds and Results from the Swedish Cyprus Expedition: A Gender Perspective at the Medelhavsmuseet, 2006.

[47] E. A. Allen, B. E. Hazen, H. C. Hoch, Y. Kwon, G. M. E. Leinhos, R. C. Staples, M. A. Stumpf, & B. T. Terhune, "Appressorium formation in response to topographical signals by 27 rust species," Phytopathology, vol. 81, no. 3, pp. 323–331, 1991.

[48] J. H. Connolly, The decomposition of red spruce sapwood by basidiomycetous fungi: extracellular matrix, calcium oxalate crystals, and cation mobilization. The University of Maine, 1996.

[49] D. Y. Vlasov, M. S. Zelenskaya, A. R. Izatulina, S. Y. Janson, & O. V. Frank-Kamenetskaya, "Oxalate crystallization under the action of brown rot fungi," Crystals, vol. 13, no. 3, p. 432, 2023.

[50] K. Pandey & A. Pitman, "FTIR studies of the changes in wood chemistry following decay by brown-rot and white-rot fungi," International biodeterioration & biodegradation, vol. 52, no. 3, pp. 151-160, 2003.

[51] C.-M. Popescu, M.-C. Popescu, & C. Vasile, "Characterization of fungal degraded lime wood by FT-IR and 2D IR correlation spectroscopy," Microchemical Journal, vol. 95, no. 2, pp. 377-387, 2010.

[52] K. Fackler & M. Schwanninger, "How spectroscopy and microspectroscopy of degraded wood contribute to understand fungal wood decay," Applied microbiology and biotechnology, vol. 96, pp. 587-599, 2012.

[53] O. Faix, "Classification of lignins from different botanical origins by FT-IR spectroscopy," 1991.

[54] O. Faix, J. Bremer, O. Schmidt, & S. J. Tatjana, "Monitoring of chemical changes in white-rot degraded beech wood by pyrolysis—gas chromatography and Fourier-transform infrared spectroscopy," Journal of Analytical and Applied Pyrolysis, vol. 21, no. 1-2, pp. 147-162, 1991.

[55] X. Colom & F. Carrillo, "Crystallinity changes in lyocell and viscose-type fibres by caustic treatment," European Polymer Journal, vol. 38, no. 11, pp. 2225-2230, 2002.

[56] R. H. Newman, "Estimation of the lateral dimensions of cellulose crystallites using 13C NMR signal strengths," Solid state nuclear magnetic resonance, vol. 15, no. 1, pp. 21-29, 1999.

[57] N. E. Marcovich, M. M. Reboredo, & M. I. Aranguren, "Modified woodflour as thermoset fillers: II. Thermal degradation of woodflours and composites," Thermochimica acta, vol. 372, no. 1-2, pp. 45-57, 2001.

[58] L. Segal, J. J. Creely, A. Martin Jr, & C. Conrad, "An empirical method for estimating the degree of crystallinity of native cellulose using the X-ray diffractometer," Textile research journal, vol. 29, no. 10, pp. 786-794, 1959.

[59] A. D. French & M. Santiago Cintrón, "Cellulose polymorphy, crystallite size, and the Segal Crystallinity Index," Cellulose, vol. 20, pp. 583-588, 2013.

[60] A. D. French, "Idealized powder diffraction patterns for cellulose polymorphs," Cellulose, vol. 21, no. 2, pp. 885-896, 2014.

[61] P. D. Manion, Tree disease concepts. 1981.

[62] D. R. Houston, Stress triggered tree diseases: the diebacks and declines. US Department of Agriculture, Forest Service, 1981.

[63] N. McDowell, W. T. Pockman, C. D. Allen, D. D. Breshears, N. Cobb, T. Kolb, J. Plaut, J. Sperry, A. West, D. G. Williams, & E. A. Yepez, "Mechanisms of plant survival and mortality during drought: Why do some plants survive while others succumb to drought?," New Phytologist, vol. 178, no. 4, pp. 719–739, 2008.

[64] W. R. Anderegg, J. M. Kane, & L. D. Anderegg, "Consequences of widespread tree mortality triggered by drought and temperature stress," Nature climate change, vol. 3, no. 1, pp. 30-36, 2013.

[65] C. I. Millar & N. L. Stephenson, "Temperate forest health in an era of emerging megadisturbance," Science, vol. 349, no. 6250, pp. 823-826, 2015.

[66] I. P. O. C. Change, "Climate change 2007: the physical science basis," Agenda, vol. 6, no. 07, p. 333, 2007.

[67] N. S. Diffenbaugh and F. Giorgi, "Climate change hotspots in the CMIP5 global climate model ensemble," Climatic change, vol. 114, pp. 813-822, 2012.

[68] G. Zittis, P. Hadjinicolaou, M. Almazroui, E. Bucchignani, F. Driouech, K. El Rhaz, L. Kurnaz, G. Nikulin, A. Ntoumos, T. Ozturk, & Y. Proestos, "Business-as-usual will lead to super and ultra-extreme heatwaves in the Middle East and North Africa," npj Climate and Atmospheric Science, vol. 4, no. 1, p. 20, 2021.

[69] R. Brázdil, P. Dobrovolný, J. Luterbacher, A. Moberg, C. Pfister, D. Wheeler, & E. Zorita, "European climate of the past 500 years: New challenges for historical climatology," Climatic Change, vol. 101, no. 1, pp. 7–40, 2010.

[70] H. A. Contreras-Cornejo, J. Larsen, S. P. Fernández-Pavía, & K. Oyama, "Climate change, a booster of disease outbreaks by the plant pathogen Phytophthora in oak forests," Rhizosphere, vol. 27, p. 100719, 2023.

[71] B. I. Cook, K. J. Anchukaitis, R. Touchan, D. M. Meko, & E. R. Cook, "Spatiotemporal drought variability in the Mediterranean over the last 900 years," Journal of Geophysical Research: Atmospheres, vol. 121, no. 5, pp. 2060-2074, 2016.

[72] H. A. A. Gaznayee, A. M. F. Al-Quraishi, K. Mahdi, J. P. Messina, S. H. Zaki, H. A. S. Razvanchy, K. Hakzi, L. Huebner, S. H. Ababakr, M. Riksen, & C. Ritsema, "Drought severity and frequency analysis aided by spectral and meteorological indices in the Kurdistan region of Iraq," Water, vol. 14, no. 19, p. 3024, 2022.

[73] M. Dubrovský, M. Hayes, P. Duce, M. Trnka, M. Svoboda, & P. Zara, "Multi-GCM projections of future drought and climate variability indicators for the Mediterranean region," Regional Environmental Change, vol. 14, pp. 1907-1919, 2014.

[74] T. Corcobado, E. Cubera, G. Moreno, & A. Solla, "Quercus ilex forests are influenced by annual variations in water table, soil water deficit and fine root loss caused by Phytophthora cinnamomi," Agricultural and forest meteorology, vol. 169, pp. 92-99, 2013.

[75] R. K. Meentemeyer, B. L. Anacker, W. Mark, & D. M. Rizzo, "Early detection of emerging forest disease using dispersal estimation and ecological niche modeling," Ecological Applications, vol. 18, no. 2, pp. 377-390, 2008.

[76] M. Kozanitas, M. R. Metz, T. W. Osmundson, M. S. Serrano, & M. Garbelotto, "The epidemiology of sudden oak death disease caused by phytophthora ramorum in a mixed bay laurel-oak woodland provides important clues for disease management," Pathogens, vol. 11, no. 2, p. 250, 2022.

[77] A. Bellahirech, M. Branco, F. X. Catry, L. Bonifácio, E. Sousa, & M. L. Ben Jamaa, "Site-and tree-related factors affecting colonization of cork oaks Quercus suber L. by ambrosia beetles in Tunisia," Annals of Forest Science, vol. 76, pp. 1-12, 2019.

[78] N. Keča, I. Koufakis, J. Dietershagen, J. A. Nowakowska, & T. Oszako, "European oak decline phenomenon in relation to climatic changes," Folia Forestalia Polonica, vol. 58, no. 3, pp. 170-177, 2016.

[79] E. Ghanbary, M. Tabari Kouchaksaraei, M. Mirabolfathy, S. Modarres Sanavi, & M. Rahaie, "Growth and physiological responses of Quercus brantii seedlings inoculated with Biscogniauxia mediterranea and Obolarina persica under drought stress," Forest Pathology, vol. 47, no. 5, p. e12353, 2017.

[80] S. Jafarnia, M. Akbarinia, B. Hosseinpour, S. Modarres Sanavi, & S. A. Salami, "Effect of drought stress on some growth, morphological, physiological, and biochemical parameters of two different populations of Quercus brantii," iForest-Biogeosciences and Forestry, vol. 11, no. 2, p. 212, 2018.

[81] A. Soge, O. Popoola, & A. Adetoyinbo, "Detection of decay and hollows in living almond trees (Terminalia catappa L. Roxb.) using electrical resistivity method," Journal of the Indian Academy of Wood Science, vol. 15, pp. 181-189, 2018.